Pharmaceutical hydrates at ambient conditions from high-pressure seeds: a case study on GABA monohydrate

ELECTRONIC SUPPLEMENTARY INFORMATION

Francesca P. A. Fabbiani, Gernot Buth, Demetrius C. Levendis, and Aurora J. Cruz-Cabeza

ffabbia@gwdg.de
aurorajosecruz@gmail.com

Contents

Experimental S1
Crystal growth S1
Crystal recovery S1
X-ray crystallography S2
CheckCIF report S3
Crystal packing description of GABA monohydrate S6
Torsion angles comparison for GABA structures deposited in the CSD S7
Details of PIXELC calculations S8
Details of the computational study S10
Crystal Structure Geometry Optimisations S10
Relative stabilities of the single-component crystals as a function of pressure S10
Relative enthalpies as a function of pressure S11
Hydration as a function of pressure S11
References S13

Experimental

Crystal growth

The title compound (Aldrich) was used directly as received. For high-pressure crystallisation experiments, aqueous solutions (6-12 M) and 2 : 1 MeOH : H_2O (4 M) were loaded in Beryllium-free diamond-anvil cells (DACs) of the Ahsbahs type (45° half-cell opening angle)[1] equipped with 600 µm culet diamonds and an Inconel gasket with a starting diameter hole of *ca.* 300 µm. On increasing pressure, precipitation of polycrystalline material was observed and a single crystal was grown by cycling the temperature inside the DAC. This general procedure is described in more detail in reference 2. The pressure inside the sample chamber was measured according to the ruby fluorescence method[3] using an in-house built kit that has an accuracy of 0.05 GPa.

Please refer to Fig. 2 of the article for an optical image of the single crystal at high pressure.

Crystal recovery

Recovery of GABA monohydrate to ambient pressure proceeded in a straightforward manner and at ambient-temperature conditions. The DAC was rapidly opened to prevent extensive dissolution and the crystal immersed in mounting oil. Subsequent to recovery, single-crystal X-ray diffraction (SXRD) data were collected at 150 K on our home diffractometer, confirming that no phase transition had taken place. For crystals grown from less concentrated solutions, prior cooling of the cell to *ca.* 288 K ensured recovered crystals were reasonably sized. The high-pressure crystallisation of GABA monohydrate was repeated several times and all crystals could be easily recovered. Recovered crystals of the monohydrate could be used to seed a saturated aqueous solution, as confirmed by SXRD. Crystals kept at 278 K under oil were stable for several months. Although no

extensive crystallisation screening was conducted, we were only able to obtain the monohydrate form with the help of hydrate seeds obtained from the high-pressure crystallisations. In the absence of these seeds, all our crystallisations at ambient conditions yielded anhydrous monoclinic GABA. At present, the possibility of obtaining the monohydrate as a transient form from low-temperature crystallisation cannot be ruled out.

Please refer to Fig. 2. of the article for optical images of the single crystal recovered to ambient conditions.

X-ray crystallography

Diffraction data were collected *in situ* at high pressure in the DAC on beamline SCD at the ANKA synchrotron source at the Karlsruhe Institute of Technology using a Bruker SMART Apex CCD diffractometer with silicon-monochromated radiation of λ = 0.7000 Å at 293 K. Data were collected with the DAC in several orientation to further improve data completeness. Data on the recovered crystal at ambient pressure were collected at 150 K on our home diffractometer, using sealed-tube radiation of λ = 0.71073 Å. High-pressure data processing was performed according to the procedure described by Dawson *et al.*[4] Data integration and global-cell refinement were performed using the program SAINT,[5] which incorporates dynamic masks to exclude the regions of the detector shaded by the pressure cell. For the high-pressure data absorption correction was applied in a two-stage procedure with the programs SHADE[6] and SADABS.[7] Data were subsequently merged using the program SORTAV,[8] as incorporated in the WinGX suite.[9] The monoclinic structure was solved by direct methods using the program SHELXS;[10] full-matrix least-squares structure refinement against F^2 was performed using SHELXL[10] through the SHELXLE GUI.[11] All non-H atoms were refined with anisotropic displacement parameters (ADPs) and soft enhanced rigid-body restraints (so-called RIGU restraints[12]) to increase the data-to-parameter ratio for the high-pressure data; refinement against an unrestrained model yielded undistinguishable results. All H-atoms could be located on difference Fourier maps: for the GABA molecule, H-atom positions were thereafter allowed to ride on their parent atom, whilst they were freely refined for the water molecule. U_{iso}(H) values were assigned in the range 1.2–1.5 times U_{eq} of the parent atom; for the low-temperature structure water U_{iso}(H) were freely refined. A final *R*-factor of 4% was obtained for the high-pressure structure, allowing a reliable description of the structural features. The fairly low completeness of *ca.* 39% is attributable to the orientation of the crystal, obtained reproducibly, and is contrasted by a very good resolution of 0.8 Å.

Crystallographic data are reported in Table S1.

Table S1. Crystallographic details for GABA monohydrate

Structure	**GABA . H_2O**	**GABA . H_2O**
Pressure	0.1 MPa	0.44 GPa
T/K	150(2)	293(2)
Space group	*C*2/*c*	*C*2/*c*
a/Å	14.3799(9)	14.276(6)
b/Å	5.6552(4)	5.6339(3)
c/Å	14.4202(9)	14.3645(10)
β/°	94.499(3)	94.598(13)
V/Å^3	1169.05(13)	1151.6(5)
D_{calc}/g cm^{-3}	1.377	1.397
d-max/Å, completeness to *d*-max	0.7, 95.1%	0.8, 39%
Measured/unique/observed reflections [a]	8128, 1669, 1305	3751, 463, 405
Parameters/restraints	82/0	80/36
R_{int}	0.026	0.051
R_1 [b]	0.038	0.04
wR [c]	0.10	0.11
$\Delta\rho_{min}/\Delta\rho_{max}$/e$^-$ Å^{-3}	-0.189/0.347	-0.096/0.122

[a] Criterion for observed reflections: $I > 2\sigma$
b $I > 2\sigma(I)$
c All data

CheckCIF report

checkCIF/PLATON report (basic structural check)
No syntax errors found. CIF dictionary
Please wait while processing .... Interpreting this report

Datablock: gaba_monohydrate_0p44_GPa

Bond precision: C-C = 0.0030 A Wavelength=0.70000
Cell: a=14.276(6) b=5.6339(3) c=14.3645(10)
alpha=90 beta=94.598(13) gamma=90
Temperature: 296 K

	Calculated	Reported
Volume	1151.6(5)	1151.6(5)
Space group	C 2/c	C 2/c
Hall group	-C 2yc	-C 2yc
Moiety formula	C4 H9 N O2, H2 O	C4 H9 N O2, H2 O
Sum formula	C4 H11 N O3	C4 H11 N O3
Mr	121.14	121.14
Dx,g cm-3	1.397	1.397
Z	8	8
Mu (mm-1)	0.113	0.118
F000	528.0	528.0
F000'	528.31	
h,k,lmax	17,7,18	7,7,17
Nref	1196	463
Tmin,Tmax		0.613,0.745
Tmin'		

Correction method= MULTI-SCAN
Data completeness= 0.387 Theta(max)= 26.120
R(reflections)= 0.0399(405) wR2(reflections)= 0.1101(463)
S = 1.068 Npar= 80

The following ALERTS were generated. Each ALERT has the format
test-name_ALERT_alert-type_alert-level.
Click on the hyperlinks for more details of the test.

Alert level A

PLAT029_ALERT_3_A _diffrn_measured_fraction_theta_full Low 0.410
RESPONSE: High-pressure data collected in the diamond-anvil cell.

Alert level C

PLAT250_ALERT_2_C Large U3/U1 Ratio for Average U(i,j) Tensor 2.4
RESPONSE: High-pressure data collected in the diamond-anvil cell. Skewing of ADPs indicative of limited region of reciprocal space sampled.

Alert level G

ABSMU01_ALERT_1_G Calculation of _exptl_absorpt_correction_mu not performed for this radiation type.
PLAT003_ALERT_2_G Number of Uiso or Uij Restrained non-H Atoms ... 7
PLAT005_ALERT_5_G No _iucr_refine_instructions_details in the CIF ? Do !
PLAT007_ALERT_5_G Note: Number of Unrefined Donor-H Atoms 3
PLAT860_ALERT_3_G Note: Number of Least-Squares Restraints 36
PLAT950_ALERT_5_G Reported and Calculated Hmax Values Differ by .. 10

1 ALERT level A = Most likely a serious problem - resolve or explain
0 ALERT level B = A potentially serious problem, consider carefully
1 ALERT level C = Check. Ensure it is not caused by an omission or oversight
6 ALERT level G = General information/check it is not something unexpected

PLATON version of 01/06/2013; check.def file version of 24/05/2013

Datablock gaba_monohydrate_0p44_GPa - ellipsoid plot

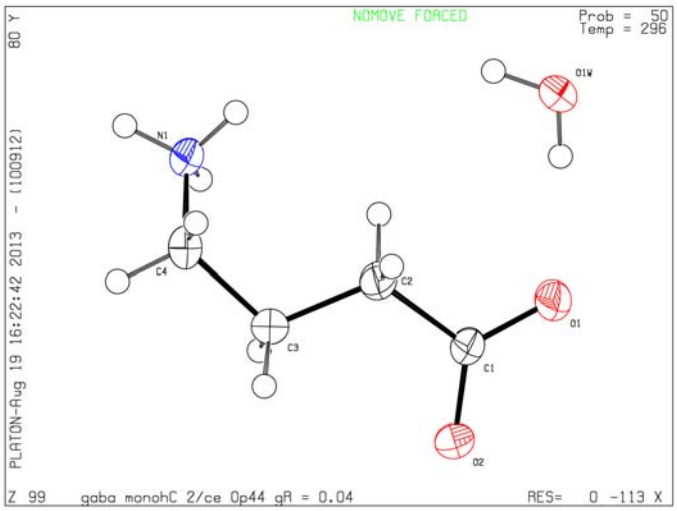

Datablock: gaba_monohydrate_150K

Bond precision: C-C = 0.0015 A Wavelength=0.71073
Cell: a=14.3799(9) b=5.6552(4) c=14.4202(9)
alpha=90 beta=94.499(3) gamma=90
Temperature: 150 K

	Calculated	Reported
Volume	1169.06(13)	1169.05(13)
Space group	C 2/c	C 2/c
Hall group	-C 2yc	-C 2yc
Moiety formula	C4 H9 N O2, H2 O	C4 H9 N O2, H2 O
Sum formula	C4 H11 N O3	C4 H11 N O3
Mr	121.14	121.14
Dx,g cm-3	1.377	1.377
Z	8	8
Mu (mm-1)	0.116	0.116
F000	528.0	528.0
F000'	528.32	
h,k,lmax	20,8,20	19,8,20
Nref	1754	1669
Tmin,Tmax	0.986,0.990	0.886,1.000
Tmin'	0.976	

Correction method= MULTI-SCAN
Data completeness= 0.952 Theta(max)= 30.406
R(reflections)= 0.0379(1305) wR2(reflections)= 0.1038(1669)
S = 1.031 Npar= 82

The following ALERTS were generated. Each ALERT has the format
test-name_ALERT_alert-type_alert-level.
Click on the hyperlinks for more details of the test.

Alert level G

PLAT005_ALERT_5_G No _iucr_refine_instructions_details in the CIF ? Do !
PLAT007_ALERT_5_G Note: Number of Unrefined Donor-H Atoms 3

---

0 **ALERT level A** = Most likely a serious problem - resolve or explain
0 **ALERT level B** = A potentially serious problem, consider carefully
0 **ALERT level C** = Check. Ensure it is not caused by an omission or oversight
2 **ALERT level G** = General information/check it is not something unexpected

---

Datablock gaba_monohydrate_150K - ellipsoid plot

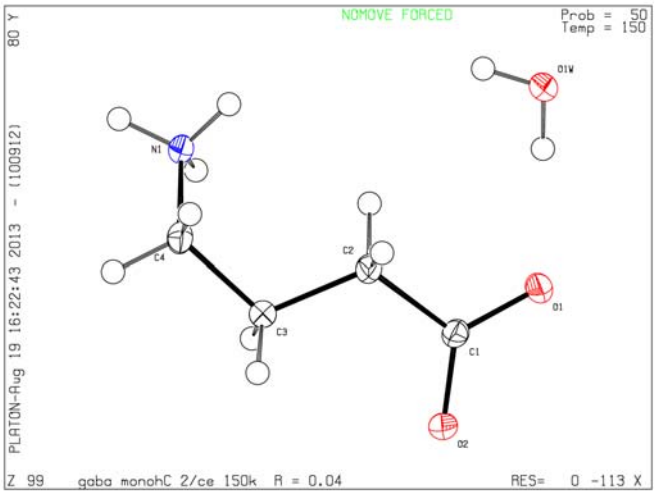

Crystal packing description of GABA monohydrate

Using graph-set notation,[13] the main building block of the crystal structure can be described as being composed of centrosymmetric $R^2_2(14)$ GABA dimers that are linked by antiparallel, hydrogen-bonded and double-stranded $C(7)$ hydrogen-bonded chains running along the *b*-axis (Fig. S1a). Each strand is strengthened by accepting two hydrogen bonds from a water molecule, which in turn links double strands related by glide symmetry. As depicted in Fig. S1b the resulting 2-D H-bonded layered structure propagates along the *c*-axis. Hydrogen-bond geometries are given in Table S2.

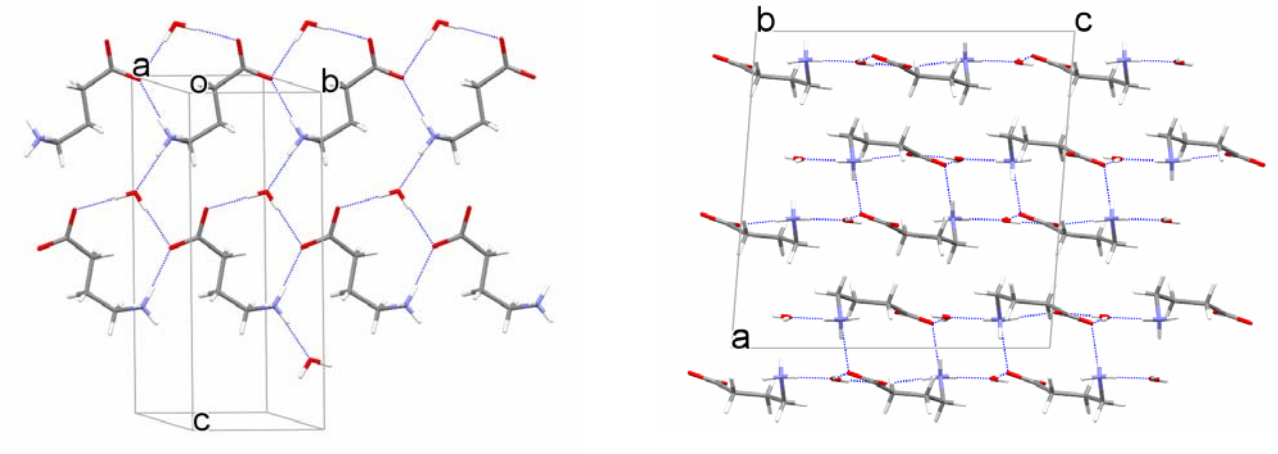

a b

Fig. S1. a) Depiction of antiparallel, hydrogen-bonded and double-stranded C(7) hydrogen-boned chains running along the *b*-axis. b) Structure viewed along the *b*-axis showing the hydrogen-bonded layered structure.

Table S2. Hydrogen-bond geometry in GABA monohydrate. Only classical hydrogen bonds are listed. Values in italics in square brackets refer to the structure from invariom refinement (see Section on PIXEL calculations).

D-H···A	D-H/Å	H···A/Å	D···A/Å	D-H···A/°
0.44 GPa structure				
N1-H1A···O2[a]	0.89	1.96	2.846(3)	176
N1-H1B···O1W[b]	0.89	1.91	2.786(3)	170
N1-H1C···O1[c]	0.89	1.97	2.844(6)	168
O1W-H1W···O1	0.84(3)	1.92(3)	2.755(2)	175(6)
O1W-H2W···O1[a]	0.84(3)	2.53(3)	3.094(2)	123(2)
O1W-H2W···O2[a]	0.84(3)	1.97(3)	2.850(2)	178(7)
150 K structure				
N1-H1A···O2[a]	0.91 [*1.02*]	1.94 [*1.83*]	2.8529(12) [*2.8536(11)*]	175 [*175*]
N1-H1B···O1W[b]	0.91 [*1.02*]	1.89 [*1.78*]	2.7917(13) [*2.7959(11)*]	171 [*171*]
N1-H1C···O1[c]	0.91 [*1.02*]	1.94 [*1.83*]	2.8383(13) [*2.8386(11)*]	170 [*169*]
O1W-H1W···O1	0.85(2) [*0.96*]	1.92(2) [*1.81*]	2.7708(13) [*2.7682(11)*]	179(2) [*179*]
O1W-H2W···O1[a]	0.84(2) [*0.96*]	2.59(2) [*2.52*]	3.1086(13) [*3.1083(11)*]	121.4(17) [*119*]
O1W-H2W···O2[a]	0.84(2) [*0.96*]	2.01(2) [*1.89*]	2.8529(12) [*2.8502(10)*]	176.8(19) [*177*]

Symmetry codes: [a] x,1+y,z; [b] x,2-y,1/2+z; [c] 1-x,1-y,1-z. All e.s.d.s calculated with the program PLATON.[14]

Torsion angles comparison for GABA structures deposited in the CSD

GABA is characterised by extensive conformational flexibility. In the literature, the conformation of the GABA molecule is typically described by the torsions about the C_1-C_α-C_β-C_γ and N-C_γ-C_β-C_α bonds (θ_2 and θ_3 in Fig. S2). These bonds can be *trans* (t, -150 to +150°), *gauche*+ (G, +30 to +90°) or *gauche*- (g, -30 to -90°). Up to nine families of conformers can be identified: gG, gg, gt, GG, Gg, Gt, tG, tg and tt. In the solid state, all structures crystallising in achiral space groups can include complementary conformers and hence the number of families simplifies to five. A further degree of freedom can be defined when the carboxylate O-atoms and ammonium H-atoms are considered (θ_1 in Fig. S2).

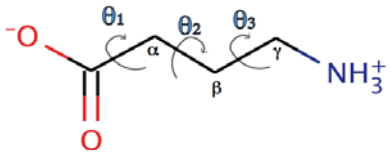

Fig. S2. Chemical diagram of the GABA zwitterion with carbon backbone naming.

The identification of stable conformers that might eventually help understanding the molecule's biological activity and selectivity has been the subject of several publications (see main article). θ_2 and θ_3, like in alkane chains, adopt their minimum energy geometries at *trans* (t, 180°), *gauche*+ (G, +60°) or *gauche*- (g, -60°). Additionally, the carboxylate group adopts its minimum energy geometry when coplanar with the alkyl chain, an *anti* geometry with $\theta_1 = 180°$. The observed conformation in the GABA monohydrate is folded, ttG [θ_1 = 163.84(10)°, θ_2 = -171.56(10)° and θ_3 = 61.31(13)° at 150 K], which amongst all structures deposited in the CSD[15] is most similar to the conformation in the anhydrous tetragonal form, gtG (Table S3).

Table S3. Torsion angles in GABA structure deposited in the CSD.

Structure	CSD ref. code	Space group	Torsion angles/° O_1-C_1-C_α-C_β [a] = θ_1	C_1-C_α-C_β-C_γ = θ_2	N-C_γ-C_β-C_α = θ_3	Conformers in the structure [b]
GABA Zwitterion						
Monoclinic	GAMBUT02	$P2_1/n$	170.90	-72.62 [c]	175.33	tgt (and tGt)
Tetragonal	GAMBUT04	$I4_1cd$	84.3(3)	-174.6(3)	-62.1(4)	Gtg (and gtG)
EtOH solvate	EYULUG	$P6_2$	-163.0(2); 172.3(3)	-175.7(3); -179.1(2)	-170.8(3); 178.0(2)	ttt
Monohydrate		$C2/c$	163.84(10)	-171.56(10)	61.31(13)	ttg (and ttG)
Protonated GABA - organics [d]						
Chloride salt	GAMBAC01	$P2_1$	-167.88	-169.28	-178.03	ttt
Benzoate salt	WERLAH	$P2_1/n$	-112.5(2)	-177.30(16)	-175.37(15)	ttt
Hemi oxalate salt	WERLEL	$P2_1/c$	108.82(13)	-61.12(15)	179.34(12)	Egt (and eGt)
Protonated GABA - organometallics						
Tin(IV) iodide	BIVMAV	$Pbca$	176.3(9)	-175.0(8)	168.2(8)	ttt
Tetrachlorocuprate(II)	IWOJEJ	$P2_1/c$	-178.3(5)	-173.5(4)	179.2(4)	ttt
Methylammonium Lead(II) iodide	QARWIQ	$C2cb$	178.5(7)	-175.0(7)	169.6(7)	ttt
Lead(II) iodide	QARWOW	$Pbca$	176.0(4)	-175.0(4)	169.4(5)	ttt

[a] This torsion angle is defined with O_1 = carboxylate O-atom closest to *anti* geometry (±180°) with respect to the carbon chain. [b] Two conformers present in structures crystallising in achiral space groups; for the only chiral space group of this series, $P6_2$, only the *trans* geometry is observed; torsion angles definition: t (*trans*, -150 to +150°), G (*gauche*, +30 to +90°), g (*gauche'*, -30 to -90°), E (*eclipsed*, +90 to +150°) and e (*eclipsed'*, -90 to -150°). [c] All e.s.d.s calculated with the program PLATON[14] for structures where the deposited CIF files contain e.s.d.s of atomic coordinates. [d] Structures containing GABA in the protonated state have been subdivided in organic structures and organometallic structures. For the latter group, only structures with GABA not coordinated to a metal centre have been considered here.

Details of PIXELC calculations

An invariom refinement using aspherical scattering factors from the invariom database[16] was performed to obtain a more precise and accurate structural model for the low-temperature structure of GABA monohydrate. By taking into account the non-spherical electron density distribution with invarioms, deconvolution of electron density and thermal motion can be achieved; this yields, amongst others, accurate bond distances (see for instance Table S2) at the cost of no extra refined parameter compared to a SHELX refinement. One of the important outcomes of this refinement procedure is that bonds to H-atoms are automatically and naturally elongated to the correct values and are not systematically short as in conventional refinement. The resulting structural model can then be taken as input for more accurate calculations of derived properties. The program XD was used for the invariom refinement.[17]

PIXELC calculations, as incorporated in the CLP program,[18] were performed to determine intermolecular interaction energies and lattice energy. PIXEL calculations allow the analysis of lattice and intermolecular interaction energies between pairs of molecules in terms of Coulombic, polarisation, dispersion and repulsion contributions. The total PIXEL energy, which is the sum of these four energy contributions, gives an indication of the overall interaction energy for a particular dimer and for crystal packing. However, it is the separation of these energies into the four different terms that makes the PIXEL method a powerful tool for crystal structure analysis.

The RETCIF, RETCOR (with the no H-atom normalisation option) and RETCHA modules of the CLP package and user input were used to prepare input files for the PIXELC calculations using a distance cut-off from the central molecule of 29 Å. The molecular electron density using the program GAUSSIAN09W[19] with the MP2/6-31G** basis set.

The coordinates of the structure from invariom refinement are as follows:

```
loop_
_atom_site_label
_atom_site_fract_x
_atom_site_fract_y
_atom_site_fract_z
O(1)    0.57832(5)     0.37091(13)    0.37540(5)
O(2)    0.61218(5)     0.11617(13)    0.49040(5)
O(1W)   0.59670(5)     0.83966(13)    0.32466(5)
N(1)    0.59006(6)     0.88511(14)    0.66321(5)
C(1)    0.60808(7)     0.32237(17)    0.45833(7)
C(2)    0.64008(7)     0.53048(18)    0.51908(6)
C(3)    0.65040(7)     0.48617(18)    0.62356(6)
C(4)    0.66889(7)     0.71293(18)    0.67908(7)
H(1A)   0.59712        0.97729        0.60313
H(1B)   0.59155        1.00092        0.71779
H(1C)   0.52794        0.79613        0.65780
H(2A)   0.59036        0.67507        0.50547
H(2B)   0.70742        0.59048        0.49755
H(3A)   0.70800        0.36278        0.63960
H(3B)   0.58661        0.40370        0.64474
H(4A)   0.67870        0.66990        0.75355
H(4B)   0.73354        0.79491        0.65868
H(1W)   0.58991        0.67634        0.34146
H(2W)   0.60411        0.92982        0.38131
```

Details for the nine energetically most significant intermolecular interaction energies are given in Table S4 and Fig. S3. Table S5 details the results of the lattice energy calculations.

Table S4. PIXELC calculations output for the nine most significant interaction energies in GABA monohydrate (150 K structure).

C_m-C_m distance/Å [a]	E_{Coul} [b]	E_{pol} [b]	E_{disp} [b]	E_{rep} [b]	$\mathbf{E_{tot}}$ [b]	Symmetry operation relating GABA molecules	Interaction type
3.590	-349.6	-102.0	-36.4	98.7	**-389.3**	inversion	**1** HB[c] dimer N1-H1C…O1
7.210	-102.0	-15.7	-7.2	10.2	**-114.7**	*c*-glide	**2** head to head dipole
4.976	-89.0	-11.9	-12.5	10.4	**-103.0**	inversion	**3** face to face dipole
4.925	-55.9	-15.3	-10.0	4.1	**-77.0**	inversion	**4** face to face dipole
5.655	-50.6	-51.9	-19.6	49.1	**-73.0**	translation along *b*	**5** HB N1-H1A…O2
6.736	-63.5	-7.0	-2.2	0.0	**-72.6**	inversion	**6** face to face dipole
5.594	-76.7	-27.2	-9.9	47.2	**-66.7**	-	**7** HB O1W-H2W…O2
3.660	-55.8	-30.0	-15.3	58.5	**-42.6**	-	**8** HB O1W-H1W…O1
4.865	-47.7	-20.3	-9.9	39.8	**-38.2**	-	**9** HB N1-H1B…O1W

[a] C_m denotes the centre of mass. [b] All energy values in kJ/mol. [c] HB denotes a hydrogen bond.

Table S5. PIXELC lattice energy calculation output for GABA monohydrate (150 K structure).

E_{Coul} [a]	E_{pol} [a]	E_{disp} [a]	E_{rep} [a]	$\mathbf{E_{tot}}$ [a]
-237.3	-72.0	-64.6	138.9	**-235.1**

[a] All energy values in kJ/mol.

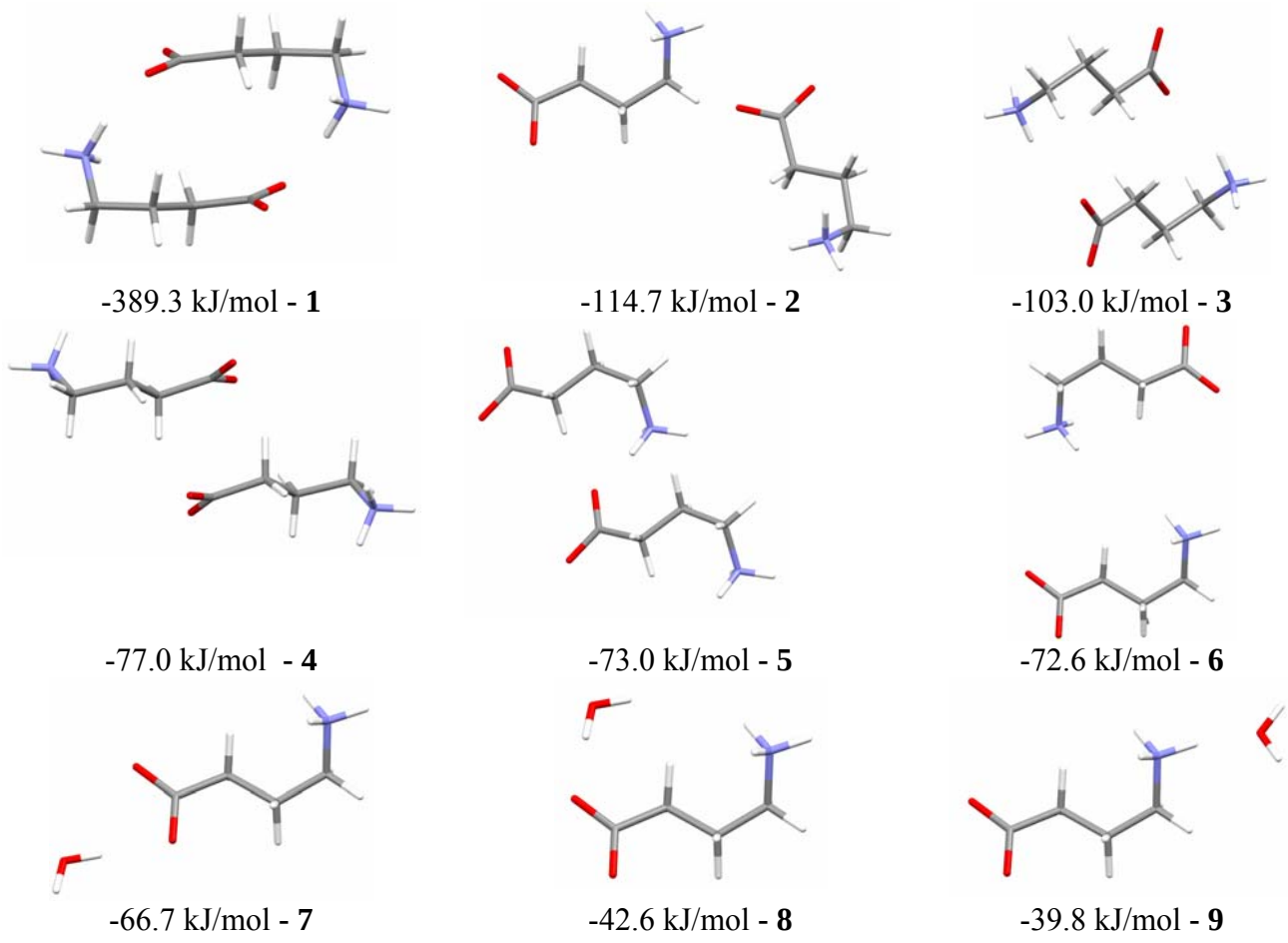

Fig. S3. The nine energetically most significant molecular pairs for GABA monohydrate (150 K structure). For interaction number, see Table S4.

Details of the computational study

Crystal Structure Geometry Optimisations

Experimentally known crystal structures were fully geometry optimised at 0.0, 0.1, 0.2, 0.3, 0.4, 0.5, 0.6, 0.7 and 0.8 GPa pressures using the program VASP.[20] The functional PBE21 was used with PAW pseudo potentials[22] and Grimme's van der Waals corrections.[23] A kinetic energy cut-off of 520 eV was used for the plane-waves. The Brillouin zone was sampled using the Monkhorst-Pack approximation[24] on a grid of k-points separated by 0.07 Å. Structural relaxation was stopped when the calculated force on every atom of the cell was less than 0.003 eV/Å.

Relative stabilities of the single-component crystals as a function of pressure

The calculations indicate that at 0 K monoclinic GABA is the most stable polymorph up to *ca.* 0.2 GPa; above this pressure, the tetragonal polymorph becomes more stable (Fig. S4). To cover the 0-0.8 GPa range at 0 K, three ordered or nearly ordered ice polymorphs were considered for the calculations, namely ice II,[25] ice IX[26] and ice XI.[27] Whilst our calculations may not accurately reproduce the enthalpies of the ice polymorphs, which are notoriously difficult to model, differences in the enthalpies of the three polymorphs over the pressure range studied are within 3 kJ/mol, in agreement with previous calculations at ambient pressure.[28] A reordering of the stability of the ice polymorphs would not have changed the hydration enthalpies significantly and neither the final conclusions drawn from the calculations.

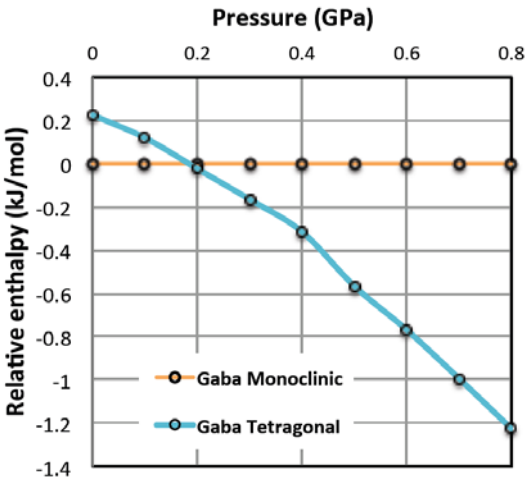

Fig. S4. Enthalpies of the GABA polymorphs, relative to the monoclinic form, as a function of pressure.

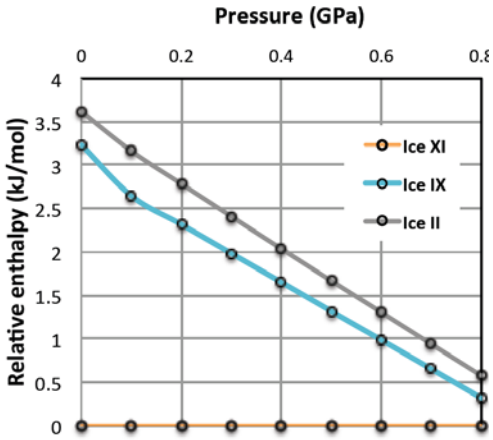

Fig. S5. Enthalpies of the ice polymorphs, relative to ice XI, as a function of pressure.

Relative enthalpies as a function of pressure

As pressure is increased, the enthalpies of the crystal structures become less stabilising because molecules are forced closer together and repulsions become more important. This is illustrated in Fig. S6. The enthalpies provided in Fig. S6 are relative to the enthalpies of each given system at 0 GPa. We can see that compression of anhydrous GABA plus ice (black) has a higher enthalpy penalty than compression of the GABA hydrate (grey). The difference between these two cases is the position of the molecule of water: in ice or inside the GABA lattice. If we compare those enthalpy penalties with those of anhydrous GABA we can estimate the cost of compressing a water molecule in the hydrate or in ice. At 0.8 GPa, for example, the relative enthalpy costs of compressing water in the GABA hydrate and in ice XI are 5 kJ/mol and 14 kJ/mol respectively (Fig. S6). This indicates that, as the pressure is increased, it is more penalising for the water molecule to be in ice than to be in the GABA hydrate.

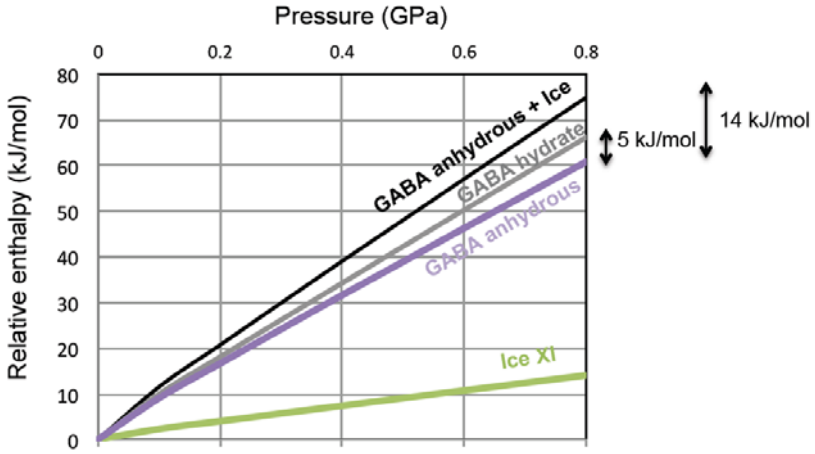

Fig. S6. Relative enthalpies of the different crystal systems as a function of pressure.

Hydration as a function of pressure

The hydration reaction can be considered as follows:

$Gaba_{crys} + Ice_{XI} \rightarrow Gaba\text{-}Hydrate_{crys} + \Delta H_{hyd}$

ΔH_{hyd} is the enthalpy of hydration and is defined, at 0K, which is the temperature at which the calculations were performed, as the difference between the enthalpy of GABA monohydrate minus the sum of the enthalpies of the most stable GABA and ice polymorphs at a given pressure [ice(XI) here]:

$\Delta H_{hyd} = H(Gaba{:}Hydrate) - [\ H(Gaba\ stable\ polymorph) + H(Ice_{IX})\ ]$

A negative ΔH_{hyd} indicates that the hydrate structure is more stable than the anhydrous form plus ice at a given set of conditions, *i.e.* that hydrate formation is driven by thermodynamics. The hydration reaction is, therefore, exothermic. Whilst recent ambient-pressure calculations have shown that cocrystal, solvate and hydrate formation (and their stoichiometries) appears to be driven by thermodynamics,[28-29] to the best of our knowledge this is the first time that such calculations have been performed under a pressure range. It is reasonable to assume that a similar driving force also occurs under high-pressure conditions, particularly given that GABA hydrate was repeatedly crystallised and grown from solution under different crystallisation conditions.

The change of the enthalpy of hydration with pressure is depicted in Fig. S7. At ambient pressures, close to 0 GPa, there is no driving force for hydrate formation (ΔH_{hyd} = ~0 kJ/mol). The enthalpy of the hydrate is equal to that of ice IX and the stable monoclinic GABA polymorph at 0 K.

As the pressure is increased, however, the hydration enthalpy becomes increasingly more negative, up to -9 kJ/mol at 0.8 GPa. Average cocrystallisation energies lie around -11 kJ/mol according to a recent study with a similar computational model.[30] Our theoretical calculations nicely corroborate the experimental observations: GABA monohydrate is obtained at pressures between 0.4-0.8 GPa, for which the ΔH_{hyd} lies between -5 up to -9 kJ/mol, and the monohydrate can be recovered to ambient pressures because it is energetically close to monoclinic GABA plus ice IX at those conditions (ΔH_{hyd} = ~0 kJ/mol). Although there is no driving force for hydrate formation at ambient conditions, if seeds of the hydrate are present in solution, growth of the hydrate occurs because the hydrate is energetically close to the unhydrated structure plus ice.

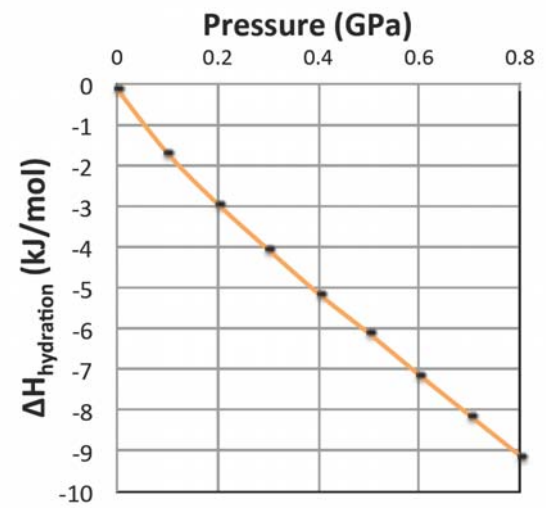

Fig. S7. Hydration enthalpy for GABA as a function of pressure.

But, what is the reason for the GABA hydrate becoming more stable than the anhydrous form plus ice at higher pressures? As the pressure is increased, the enthalpies of all the involved forms become less stabilising because molecules are forced closer together and repulsions become more important (Fig. S6). We noticed that compressing water within ice costs relatively more energy than compressing water within the GABA monohydrate structure. Compression of a water molecule in ice from 0 to 0.8 GPa occurs at a structural cost of shortening 4 H-bonds by 0.035 Å each and an enthalpic cost of 14 kJ/mol. In contrast, compression of water within the GABA hydrate from 0 to 0.8 GPa occurs at a structural cost of shortening 3 H-bonds by an average of 0.019 Å each and an estimated enthalpic cost of 5 kJ/mol. Hence, this indicates that because of the poorer compressibility of water within ice,[31] hydration of GABA becomes thermodynamically favoured at higher pressures. This is likely to be the case for many other pharmaceuticals; in fact, high-pressure crystallisations are known to produce hydrates otherwise unseen under ambient conditions.[32] Whether those hydrates can be recoverable to ambient pressures and be used as seeds may be indeed anticipated with the calculations presented herein.

References

[1] H. Ahsbahs, *Z. Kristallogr*, 2004, **219**, 305; H. Ahsbahs, *Z. Kristallogr. Suppl.*, 1995, **9**, 42.
[2] F. P. A. Fabbiani and C. R. Pulham, *Chem. Soc. Rev.*, 2006, **35**, 932,
[3] G. J Piermarini, S. Block, J. D. Barnett and R.A. Forman, *J. Appl. Phys.*, 1975, **46**, 2774.
[4] A. Dawson, D. R. Allan, S. Parsons and M. Ruf, *J. Appl. Cryst*., 2004, **37**, 410.
[5] Bruker-Nonius, SAINT version 7.32A, 2006, Bruker-AXS, Madison, Wisconsin, USA.
[6] S. Parsons, SHADE, 2004, The University of Edinburgh, Edinburgh, United Kingdom.
[7] G. M. Sheldrick, SADABS Version 2008-1, 2008, Bruker-AXS, Madison, Wisconsin, USA.
[8] R. H. Blessing, *Acta Crystallogr. Sect. A Found. Crystallogr.*, 1995, **51**, 33.
[9] L. J. Farrugia, *J. Appl. Cryst*., 2012, **45**, 849.
[10] G. M. Sheldrick, *Acta Crystallogr. Sect. A Found. Crystallogr.*, 2008, **64**, 112.
[11] C. B. Hübschle, G. M. Sheldrick and B. Dittrich, *J. Appl. Cryst*., 2012, **44**, 1281.
[12] A. Thorn, B. Dittrich and G. M. Sheldrick., *Acta Crystallogr. Sect. A Found. Crystallogr.*, 2012, **68**, 448.
[13] M. C. Etter, *Acc. Chem. Res.*, 1990, **23**, 120; M. C. Etter, J. C. MacDonald and J. Bernstein, *Acta Crystallogr. Sect. B Struct. Sci.*, 1990, **46**, 256.
[14] A. L. Spek, *Acta Crystallogr. Sect. D Biol. Crystallogr.*, 2009, **65**, 148.
[15] F. H. Allen, *Acta Crystallogr. Sect. B Struct. Sci.*, 2002, **58**, 380.
[16] B. Dittrich, T. Koritsánszky and P. Luger, *Angew. Chem., Int. Ed.*, 2004, **43**, 2718; B. Dittrich, C. B. Hübschle, M. Messerschmidt, R. Kalinowski, D. Girnt. and P. Luger, *Acta Crystallogr. Sect. A Found. Crystallogr*., 2005, **61**, 314.
[17] A. Volkov, P. Macchi, L. J. Farrugia, C. Gatti, P. R. Mallinson, T. Richter and T. Koritsánszky, XD2006 – a computer program for multipole refinement, topological analysis and evaluation of intermolecular energies from experimental and theoretical structure factors, University at Buffalo, NY, USA; University of Milano, Italy; University of Glasgow, UK; CNRISTM, Milano, Italy; Middle Tennessee State University, TN, USA, 2006.
[18] A. Gavezzotti, *New J. Chem.*, 2001, **35**, 1360.
[19] M. J. Frisch, G. W. Trucks, H. B. Schlegel, G. E. Scuseria, M. A. Robb, J. R. Cheeseman, G. Scalmani, V. Barone, B. Mennucci, G. A. Petersson, H. Nakatsuji, M. Caricato, X. Li, H. P. Hratchian, A. F. Izmaylov, J. Bloino, G. Zheng, J. L. Sonnenberg, M. Hada, M. Ehara, K. Toyota, R. Fukuda, J. Hasegawa, M. Ishida, T. Nakajima, Y. Honda, O. Kitao, H. Nakai, T. Vreven, J. A. Montgomery, Jr., J. E. Peralta, F. Ogliaro, M. Bearpark, J. J. Heyd, E. Brothers, K. N. Kudin, V. N. Staroverov, R. Kobayashi, J. Normand, K. Raghavachari, A. Rendell, J. C. Burant, S. S. Iyengar, J. Tomasi, M. Cossi, N. Rega, J. M. Millam, M. Klene, J. E. Knox, J. B. Cross, V. Bakken, C. Adamo, J. Jaramillo, R. Gomperts, R. E. Stratmann, O. Yazyev, A. J. Austin, R. Cammi, C. Pomelli, J. W. Ochterski, R. L. Martin, K. Morokuma, V. G. Zakrzewski, G. A. Voth, P. Salvador, J. J. Dannenberg, S. Dapprich, A. D. Daniels, Ö. Farkas, J. B. Foresman, J. V. Ortiz, J. Cioslowski and D. J. Fox GAUSSIAN09W, Gaussian, Inc., Wallingford, Connecticut, USA, 2009
[20] G. Kresse and J. Hafner, *J. Phys. Rev. B*, 1993, **47**, 558; G. Kresse and J. Hafner, *J. Phys. Rev. B*, 1994, **49**, 14251; G. Kresse and J. Furthmüller, *Comput. Mater. Sci*..,1996, **6**, 15; G. Kresse and J. Furthmüller, *Phys. Rev. B*, 1996, **54**, 11169.
[21] J. P. Perdew, K. Burke and M. Ernzerhof, *Phys. Rev. Lett.*, 1996, **77**, 3865.
[22] P. E. Blöchl, *Phys. Rev. B*, 1994, **50**, 17953; G. Kresse and D. Joubert, *Phys. Rev. B*, 1999, **59**, 1758.
[23] S Grimme, *J. Comput. Chem.*, 2006, **27**, 1787.
[24] H. J. Monkhorst and J. D. Pack, *Phys. Rev. B*, 1976, **13**, 5188–5192.
[25] B. Kamb, *Acta Crystallogr*., 1964, **17**, 1437.
[26] S. J. La Placa, W. C. Hamilton, B. Kamb and A. Prakash, *J. Chem. Phys.*,1972, **58**, 567.
[27] A. J. Leadbetter, R. C. Ward, J. W. Clark, P. A. Tucker, T. Matsuo and H. Suga, *J. Phys. Chem.*, 1985, **82**, 424.
[28] A. T. Hulme and S. L. Price, *J. Chem. Theor. Comput.*, 2007, **3**, 1597; D. E. Braun, P. G. Karamertzanis and S. L. Price, *Chem. Commun.*, 2011, **47**, 5443.
[29] A. J. Cruz-Cabeza, G. M. Day, W. D. S. Motherwell and W. Jones, *J. Am. Chem. Soc.*, 2006, **128**, 14466; A. J. Cruz-Cabeza, G. M. Day and W. Jones, *Chem. Eur. J.*, 2008, **14**, 8830; A. J. Cruz-Cabeza, S. Karki, L. Fábián, T. Friščić, G. M. Day and W. Jones, *Chem. Commun.*, 2010, **46**, 2224.
[30] S. Chan, J. Kendrick, M. A. Neumann and F. Leusen, *CrystEngComm*, 2013, **15**, 3799.
[31] C. Q. Sun, X. Zhang and W. Zheng, *Chem. Sci.*, 2012, **3**, 1455..
[32] F. P. A. Fabbiani, D. R. Allan, W. G. Marshall, S. Parsons, C. R. Pulham and R. I. Smith, *J. Cryst. Growth*, 2004, **275**(1-2), 185; H. Tomkowiak, A. Olejniczak and A. Katrusiak, *Cryst. Growth Des.*, 2013, **13**(1), 121; A. Olejniczak and A. Katrusiak, *Cryst. Growth Des.*, 2011, **11**(6), 2250; F. P. A. Fabbiani, D. R. Allan, W. I. F. David, S. A. Moggach and C. R. Pulham, *CrystEngComm*, 2004, **6**(82), 504; I. D. H. Oswald, I. Chataigner, S. Elphick, F. P. A. Fabbiani, A. R. Lennie, J. Maddaluno, W. G. Marshall, C. R. Pulham, T. J. Prior and R. I. Smith, *CrystEngComm*, 2009, **11**, 359; F. P. A. Fabbiani, D. R. Allan, W. I. F. David, A. J. Davidson, A. R. Lennie, S. Parsons, C. R. Pulham and J. E. Warren, *Cryst. Growth Des.*, 2007, **7**, 1115; F. P. A. Fabbiani, B. Dittrich, A. J. Florence, T. Gelbrich, M. B. Hursthouse, W. F. Kuhs, N. Shankland and H. Sowa, *CrystEngComm*, 2009, **11**, 1396; F. P. A. Fabbiani, D. C. Levendis, G. Buth, W. F. Kuhs, N. Shankland and H. Sowa, *CrystEngComm*, 2010, **12**, 2354.